Varszegi B., Takacs D., Stepan G., Hogan S. J.: Stabilizing skateboard speed-wobble with reflex delay, *Journal of the Royal Society Interface* **13**, 20160345, (2016) doi: 10.1098/rsif.2016.0345

Stabilizing Skateboard Speed-wobble with Reflex Delay

Balazs Varszegi[1], Denes Takacs[2], Gabor Stepan[3], S. John Hogan[4]

Keywords:
nonholonomic mechanics, human balancing, skateboard, time delay

Abstract:
A simple mechanical model of the skateboard-skater system is analysed, in which the effect of human control is considered by means of a linear proportional-derivative (PD) controller with delay. The equations of motion of this nonholonomic system are neutral delay-differential equations. A linear stability analysis of the rectilinear motion is carried out analytically. It is shown how to vary the control gains with respect to the speed of the skateboard to stabilize the uniform motion. The critical reflex delay of the skater is determined as the function of the speed. Based on this analysis, we present an explanation for the linear instability of the skateboard-skater system at high speed. Moreover, the advantages of standing ahead of the centre of the board is demonstrated from the view point of reflex delay and control gain sensitivity.

1 Introduction

Skateboarding became a popular sport all over the word after the construction of the first commercial skateboard in the 1950's. Nowadays, the skateboards is considered both as a vehicle and as an item of sport equipment but it is also represents a kind of lifestyle. Two decades after the skateboard was merchandised, the first mechanical model was presented by Hubbard [1, 2]. He demonstrated that the dynamical behaviour of the skateboard shows many interesting phenomena. Subsequent, the mechanics of skateboarding became a popular research field among engineers and physicists studying nonholonomic systems. Hubbard's model of skateboarding was improved by Kremnev and Kuleshov [3], and has been further developed by many researchers.

All of these studies showed that the stabilization of the rectilinear motion (rolling along a straight line) gets easier as the longitudinal speed increases. Similar observations were used by Wisse and Schwab [4] to explain the stability properties of the bicycle and the three-dimensional biped walking machine. The corresponding stability properties are also relevant in robotic locomotion (see [5] or [6]). However, research on the dynamics of nonholonomic systems is far from being concluded. Recent publications on the lateral stability and the longitudinal dynamics of bicycles present many new aspects of applied nonholonomic systems (see in [7, 8, 9]); similarly, research on skateboard dynamics has uncovered many new phenomena.

For example, the loss of stability of steady-state rectilinear skateboarding is also observed in practice at high speeds. This behaviour of the skateboard has not been explained by the traditional mechanical models. The standard models did not consider the essential interaction between the nonholonomic skateboard and the human control. Even if a complex model of human control is applied to skateboarding [10], the reflex time of the operator is neglected. The human reflex time in the control loop plays an essential role in dynamical systems, as has been shown in many studies on human balancing. These papers investigate the problem both from the biological and engineering points of view (see, for example, Milton et al [11], Stepan [12] or Chagdes et al [13]). Consequently, the interactions between mechanical systems and human operators offer interesting research topics; while the mathematical modelling of the mechanical part is well developed and understood, the complexity of the human control with its sensors and actuators still requires further analysis.

In this paper, a mechanical model of the skateboard is constructed in which the effect of human control is taken into account. We consider the simplest possible linear proportional-derivative (PD) control with human reflex delay in order to actuate a torque at the skater's ankle. The most compact equations of motion of this controlled nonholonomic system are derived using the Gibbs-Appell equations (see Gantmacher [14]). The stability analysis of the rectilinear motion is investigated analytically, and a case study is shown to represent the practical consequences of the results.

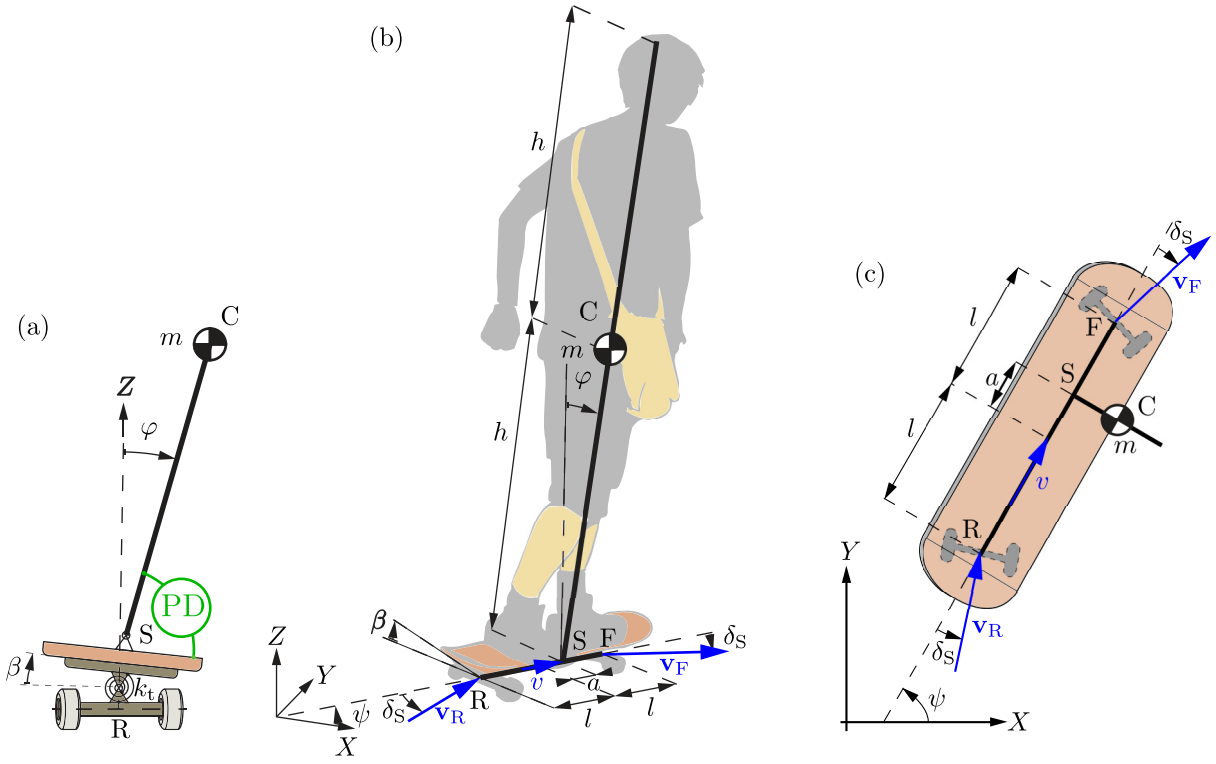

Figure 1: The simplified mechanical model of the skateboard-skater system based on [3, 15]; panel (a) shows the rear view of the system, panel (b) shows an isometric one, while panel (c) shows the top one.

2 Mechanical model

The mechanical model (see figure 1) is a simplified version of [3] and [15] with a control torque added to model the balancing effort of the skater. The skateboard is modelled by a massless rod between the points F (front) and R (rear) in figure 1 while the skater is represented by another massless rod between the points S (skateboard actuation point) and C (mass centre of skater) with a lumped mass m at its free end C. These two rods are connected by a hinge at the point S. Further parameters are as follows: $2h$ denotes the height of the skater, $2l$ is the length of the board, a characterizes the location of the skater on the board (where $a > 0$ means that the skater stands ahead of the centre of the board), m represents the mass of the skater and g is the acceleration of gravity. Both the mass and the mass moment of inertia of the board are neglected.

We assume that the skateboard wheels are always in contact with the ground. Consequently, the longitudinal axis of the skateboard is always parallel to the ground. The described geometry requires five generalised coordinates to describe the motion; we choose x and y as the horizontal coordinates of the point S; ψ denotes the longitudinal direction of the skateboard; φ is the deflection angle of the skater from the vertical; and finally, β is the deflection angle of the board about the rod FR.

As shown in figure 1, the rotation of the skateboard about its longitudinal axis is counteracted by the torsional spring of stiffness k_t, which is installed in the special wheel suspension system of the skateboard. The rotation of the skater around the longitudinal axis of the skateboard is opposed. by the PD controlled internal torque generated by the skater. Since, rectilinear motion is considered as the desired motion, zero torque is produced by the controller when the deflection angle of the skater is zero (i.e. $\varphi = 0$). Thus, the control torque can be modelled by

$$M_{\mathrm{PD}}(t) = p\varphi(t-\tau) + d\dot{\varphi}(t-\tau) \tag{1}$$

where τ refers to the reflex time (time delay) of the human control, p and d represent the proportional and the differential control gains, respectively.

Regarding the rolling wheels of the skateboard, kinematic constraints can be given for the velocities $\mathbf{v}_F$, $\mathbf{v}_R$ of points F and R. The directions of the velocities of these points depend on the deflection angle β of the board

[1]Department of Applied Mechanics, Budapest University of Technology and Economics, Budapest, Hungary, e-mail: varszegi@mm.bme.hu
[2]MTA-BME Research Group on Dynamics of Machines and Vehicles, Budapest, Hungary, e-mail: takacs@mm.bme.hu
[3]Department of Applied Mechanics, Budapest University of Technology and Economics, Budapest, Hungary, e-mail: stepan@mm.bme.hu
[4]Department of Engineering Mathematics, University of Bristol, Bristol, United Kingdom, e-mail: S.J.Hogan@bristol.ac.uk

through the so-called steering angle δ_S (see figure 1). This connection can be described by the expression:

$$\sin\beta\cot\kappa = \tan\delta_S \tag{2}$$

where the constant κ is the so-called rake angle in the skateboard wheel suspension system (see figure 2, where the steering mechanism of the skateboard is illustrated). Steering works as follows: as the skater deflects the board by an angle β, the axes of the wheels turn through an angle δ_S given by (2) according to the geometric constraints of the steering mechanism. Namely, the axles of the wheels are always parallel to the ground, and are perpendicular to the king pin axis characterized by the unit vector $\mathbf{e}_{DK}$ in figure 2, which rotates together with the board. More details on the steering mechanism of skateboards can be found in [1, 10].

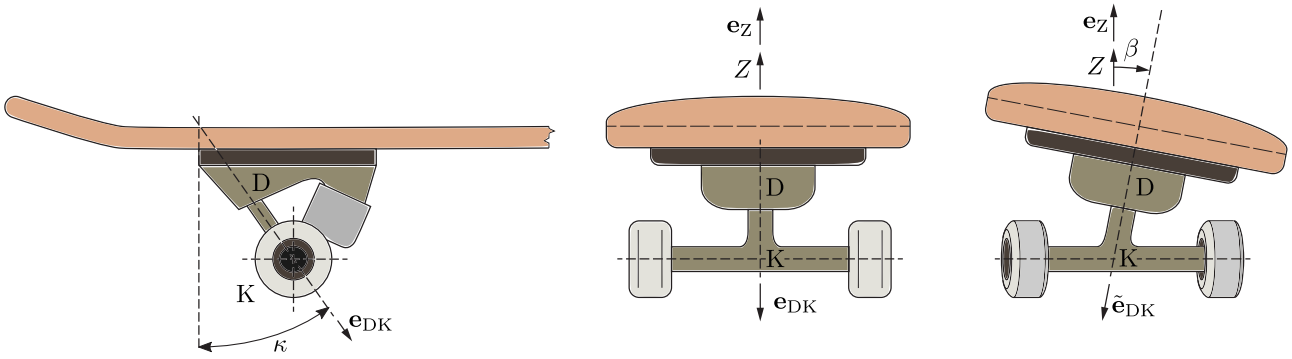

Figure 2: Skateboard wheel suspension system

Since the directions of the velocities of F and R are constrained (see Fig 1.b), two scalar kinematic constraints can be constructed:

$$(\cos\psi\sin\beta\cot\kappa - \sin\psi)\,\dot{x} + (\sin\psi\sin\beta\cot\kappa + \cos\psi)\,\dot{y} + (l-a)\,\dot{\psi} = 0\,, \tag{3a}$$

$$(\cos\psi\sin\beta\cot\kappa + \sin\psi)\,\dot{x} + (\sin\psi\sin\beta\cot\kappa - \cos\psi)\,\dot{y} + (l+a)\,\dot{\psi} = 0\,. \tag{3b}$$

We also introduce a third kinematic constraint, namely, the longitudinal speed v of the board is assumed to be constant:

$$\dot{x}\cos\psi + \dot{y}\cos\psi = v \tag{4}$$

It can be shown that this constraint does not influence the linear stability of the rectilinear motion of the skateboard. Nevertheless, it makes our equations simpler in spite of the fact that the system is not conservative any more.

All of the kinematic constraints (Eq. (3) and (4)) are linear combinations of the generalised velocities, so they can be written in the following matrix form:

$$\begin{bmatrix} \cos\psi\sin\beta\cot\kappa - \sin\psi & \sin\psi\sin\beta\cot\kappa + \cos\psi & -a+l & 0 & 0 \\ \cos\psi\sin\beta\cot\kappa + \sin\psi & \sin\psi\sin\beta\cot\kappa - \cos\psi & a+l & 0 & 0 \\ \cos\psi & \sin\psi & 0 & 0 & 0 \end{bmatrix} \begin{bmatrix} \dot{x} \\ \dot{y} \\ \dot{\psi} \\ \dot{\varphi} \\ \dot{\beta} \end{bmatrix} = \begin{bmatrix} 0 \\ 0 \\ v \end{bmatrix}. \tag{5}$$

The equations of motion of this nonholonomic system can be derived efficiently by means of the Gibbs-Appell equations [14]. This approach is often used in vehicle dynamics [16] or even in case of skateboards [17] since it leads to the most compact mathematical form having advantages in case of analytical studies. Several other methods like Newton's Second Law of motion with constraint forces, Lagrange-d'Alembert equations with constraint forces [18] or Kane's equations [19] lead to equivalent results. Reference [16] contains an electronic supplement where the detailed derivation and application of the Gibbs-Appell equations are presented.

In order to use this approach, pseudo velocities have to be chosen, by which the kinematic constraints can be taken into account with a minimum number of coordinates. In our case, two pseudo velocities σ_1 and σ_2 are needed since this is the difference between the 5 generalised coordinates and the 3 kinematic constraints. We take σ_1, σ_2 to be the angular velocities of the skater and the skateboard around the longitudinal axis, respectively:

$$\sigma_1 := \dot{\varphi} \quad \text{and} \quad \sigma_2 := \dot{\beta}\,. \tag{6}$$

The generalised velocities can be expressed with the help of the two pseudo velocities and the five generalised

coordinates:

$$\begin{bmatrix} \dot{x} \\ \dot{y} \\ \dot{\psi} \\ \dot{\varphi} \\ \dot{\beta} \end{bmatrix} = \begin{bmatrix} v\left(\cos\psi + \frac{a}{l}\cot\kappa\sin\beta\sin\psi\right) \\ v\left(\sin\psi - \frac{a}{l}\cot\kappa\sin\beta\cos\psi\right) \\ -\frac{v}{l}\cot\kappa\sin\beta \\ \sigma_1 \\ \sigma_2 \end{bmatrix}. \tag{7}$$

Taking the time derivatives of both sides, the generalised accelerations can be expressed by pseudo accelerations, pseudo velocities and general coordinates.

During the derivation of the equation of motion, the so-called energy of acceleration ($\mathcal{A}$) has to be determined. For a lumped mass it can be computed as:

$$\mathcal{A} = \frac{1}{2} m\, \mathbf{a}_\mathrm{C} \cdot \mathbf{a}_\mathrm{C} \tag{8}$$

where $\mathbf{a}_\mathrm{C}$ is the acceleration of the lumped mass:

$$\mathbf{a}_\mathrm{C} = \begin{bmatrix} \ddot{x} + h\sin\psi\left(\ddot{\varphi}\cos\varphi - \left(\dot{\varphi}^2 + \dot{\psi}^2\right)\sin\varphi\right) + h\cos\psi\left(2\dot{\varphi}\dot{\psi}\cos\varphi + \ddot{\psi}\sin\varphi\right) \\ \ddot{y} + h\sin\varphi\left(\ddot{\psi}\sin\psi + \left(\dot{\varphi}^2 + \dot{\psi}^2\right)\cos\psi\right) + h\cos\varphi\left(2\dot{\varphi}\dot{\psi}\sin\psi + \ddot{\psi}\cos\psi\right) \\ -h\left(\dot{\varphi}^2\cos\varphi + \ddot{\varphi}\sin\varphi\right) \end{bmatrix} \tag{9}$$

We introduce dimensionless geometric parameters and frequency-like physical parameters:

$$\omega_1 = \sqrt{\frac{g}{h}}, \quad V = \frac{v}{\sqrt{gh}} = \frac{v}{h\omega_1}, \quad A = \frac{a}{L} = \frac{a\cot\kappa}{l}, \quad H = \frac{h}{L} = \frac{h\cot\kappa}{l}, \tag{10}$$

which simplifies the subsequent analysis. For example, ω_1 is the natural angular frequency of a pendulum originating in our system. Clearly, our system simplifies to a simple spring-supported inverted pendulum if the longitudinal speed is zero ($v = 0$). Using these new parameters and the previously determined acceleration (9) of point C, in which the generalised accelerations and velocities are replaced by the pseudo accelerations and pseudo velocities from the time derivatives of exp. (7), we obtain:

$$\frac{1}{mh^2}\mathcal{A} = \frac{1}{2}\dot{\sigma}_1^2 + \left(V\cos\varphi\left(HV\sin\beta + A\frac{\sigma_2}{\omega_1}\cos\beta\right) - \frac{1}{2}V^2H^2\sin(2\varphi)\sin^2\beta\right)\omega_1^2\dot{\sigma}_1 + \dots, \tag{11}$$

where the dots refer to the part of the expression, which does not contain pseudo accelerations and has no relevance later.

The Gibbs-Appell equations assume the form

$$\frac{\partial\mathcal{A}}{\partial\dot{\sigma}_i} = \Gamma_i, \quad i = 1, 2, \tag{12}$$

where Γ_i is the pseudo force related to the pseudo velocity σ_i. It can be determined from the virtual power of the active forces:

$$\delta P = \mathbf{G}\cdot\delta\mathbf{v}_\mathrm{C} + \mathbf{M}_\mathrm{PD}\cdot\delta\omega_\mathrm{s} + (-\mathbf{M}_\mathrm{PD})\cdot\delta\omega_\mathrm{b} + \mathbf{M}_{k_\mathrm{t}}\cdot\delta\omega_\mathrm{b} = \Gamma_1\delta\sigma_1 + \Gamma_2\delta\sigma_2, , \tag{13}$$

where

$$\mathbf{G} = \begin{bmatrix} 0 & 0 & -mg \end{bmatrix}^\mathrm{T} \tag{14}$$

is the gravitational force, $\mathbf{v}_\mathrm{C}$ is the velocity of point C,

$$\mathbf{M}_\mathrm{PD} = \begin{bmatrix} -M_\mathrm{PD}\cos\psi & -M_\mathrm{PD}\sin\psi & 0 \end{bmatrix}^\mathrm{T} \tag{15}$$

is the torque vector produced by the controller, and

$$\boldsymbol{\omega}_\mathrm{s} = \begin{bmatrix} \dot{\varphi}\cos\psi & \dot{\varphi}\sin\psi & \dot{\psi} \end{bmatrix}^\mathrm{T} \quad \text{and} \quad \boldsymbol{\omega}_\mathrm{b} = \begin{bmatrix} \dot{\beta}\cos\psi & \dot{\beta}\sin\psi & \dot{\psi} \end{bmatrix}^\mathrm{T} \tag{16}$$

are the angular velocities of the skater and the board, respectively. Finally

$$\mathbf{M}_{k_\mathrm{t}} = \begin{bmatrix} -k_\mathrm{t}\varphi\cos\psi & -k_\mathrm{t}\varphi\sin\psi & 0 \end{bmatrix}^\mathrm{T} \tag{17}$$

is the torque produced by the spring in the suspension of the board. The notation δ refers to virtual quantities. After substitution, we obtain

$$\delta P = (mgh\sin\varphi - M_\mathrm{PD})\,\delta\dot{\varphi} + (M_\mathrm{PD} - k_\mathrm{t}\beta)\,\delta\dot{\beta}. \tag{18}$$

which leads to the two pseudo forces

$$\Gamma_1 = mgh\sin\varphi - M_{\mathrm{PD}} \quad \text{and} \quad \Gamma_2 = M_{\mathrm{PD}} - k_{\mathrm{t}}\beta\,, \tag{19}$$

Now, both sides of equation (12) can be calculated, and due to the fact, that the energy of acceleration does not depend on the derivative of second pseudo velocity σ_2 the Gibbs-Appell equations assume the simple form

$$\frac{\dot{\sigma}_1}{\omega_1^2} + V\cos\varphi\left(HV\sin\beta + A\frac{\sigma_2}{\omega_1}\cos\beta\right) - \frac{1}{2}V^2H^2\sin(2\varphi)\sin^2\beta = \sin\varphi - \frac{M_{\mathrm{PD}}}{\omega_1^2 mh^2}\,, \tag{20a}$$

$$0 = \frac{M_{\mathrm{PD}}}{\omega_1^2 mh^2} - K\beta\,, \tag{20b}$$

where the dimensionless quantity K is given by

$$K = \frac{\omega_2^2}{\omega_1^2} = \frac{k_t}{mgh} \quad \text{and} \quad \omega_2 = \sqrt{\frac{k_{\mathrm{t}}}{mh^2}}\,. \tag{21}$$

Since the mass and the mass moment of inertia of the board are neglected, Eqn. (20b) corresponds to torque balancing equation, from which the board deflection angle β can be expressed as a function of the control torque:

$$\beta = P\varphi(t-\tau) + \frac{D}{\omega_1}\dot{\varphi}(t-\tau)\,, \tag{22}$$

where the dimensionless control parameters are:

$$P = \frac{p}{k_t} \quad \text{and} \quad D = \frac{d}{k_t}\omega_1\,. \tag{23}$$

Consequently, β and $\sigma_2 = \dot{\beta}$ can be eliminated and the system can be described uniquely with four generalized coordinates: x, y, ψ, φ and only one pseudo velocity σ_1.

Considering the first equation of the Gibbs-Appell equations (20a) and the expression of β in (22) with the expressions of the general velocities (7), we obtain the governing equation of the system (hereafter we set $\sigma = \sigma_1$). These equations can be rearranged to become:

$$\frac{\dot{\sigma}}{\omega_1^2} = HV^2\left(\frac{H}{2}\sin(2\varphi)\sin^2\left(P\varphi(t-\tau) + \frac{D}{\omega_1}\sigma(t-\tau)\right) - \cos\varphi\sin\left(P\varphi(t-\tau) + \frac{D}{\omega_1}\sigma(t-\tau)\right)\right) + \sin\varphi + \tag{24a}$$

$$- \frac{AV\left(P\sigma(t-\tau) + \frac{D}{\omega_1}\dot{\sigma}(t-\tau)\right)}{\sqrt{\omega_1^2 + \left(\omega_1 P\varphi(t-\tau) + D\sigma(t-\tau)\right)^2}}\cos\varphi\cos\left(P\varphi(t-\tau) + \frac{D}{\omega_1}\sigma(t-\tau)\right) - K\left(P\varphi(t-\tau) + \frac{D}{\omega_1}\sigma(t-\tau)\right)\,,$$

$$\dot{\varphi} = \sigma\,, \tag{24b}$$

$$\frac{\dot{x}}{h} = V\omega_1\left(\cos\psi + A\sin\psi\sin\left(P\varphi(t-\tau) + \frac{D}{\omega_1}\sigma(t-\tau)\right)\right)\,, \tag{24c}$$

$$\frac{\dot{y}}{h} = V\omega_1\left(\sin\psi - A\cos\psi\sin\left(P\varphi(t-\tau) + \frac{D}{\omega_1}\sigma(t-\tau)\right)\right)\,, \tag{24d}$$

$$\dot{\psi} = -HV\omega_1\sin\left(P\varphi(t-\tau) + \frac{D}{\omega_1}\sigma(t-\tau)\right)\,. \tag{24e}$$

Note that x, y and ψ are cyclic coordinates, so only the first two equations ((24a) and (24b)) of the system (24) of differential equations describe the essential motion. If these are solved then the hidden motion can be directly integrated for the cyclic generalized coordinates.

3 Stability analysis

In this section we are going to investigate the linear stability of the steady-state rectilinear motion of the skateboard-skater system. First, we take the linearised equation of motion around the trivial solution with respect to small perturbations in σ and φ. This results in a linear neutral delay-differential equation (NDDE)

$$\dot{\mathbf{X}}(t) = \mathbf{J}\mathbf{X}(t) + \mathbf{T}_0\mathbf{X}(t-\tau) + \mathbf{T}_1\dot{\mathbf{X}}(t-\tau)\,, \tag{25}$$

where

$$\mathbf{J}=\begin{bmatrix}0 & \omega_1^2\\ 1 & 0\end{bmatrix},\quad \mathbf{T}_0=\begin{bmatrix}-\omega_1\left(APV+D\left(K+HV^2\right)\right) & -\omega_1^2P\left(K+HV^2\right)\\ 0 & 0\end{bmatrix},$$
$$\mathbf{T}_1=\begin{bmatrix}-DAV & 0\\ 0 & 0\end{bmatrix},\quad \mathbf{X}\left(t\right)=\begin{bmatrix}\sigma(t)\\ \varphi(t)\end{bmatrix}. \tag{26}$$

The stability investigation of a linear NDDE can be handled by means of Laplace transforms [20], which is equivalent to the substitution of the exponential trial solution $\mathbf{X}\left(t\right)=\mathbf{K}\mathrm{e}^{\lambda\omega_1 t}$, where $\mathbf{K}\in\mathbb{C}^2$ and $\lambda\in\mathbb{C}$ is the dimensionless characteristic exponent. With new rescaled parameters

$$\tilde{\tau}=\tau\omega_1\,,\quad \tilde{D}=D\left(K+HV^2\right)\,,\quad \tilde{P}=P\left(K+HV^2\right)\,,\quad U=\frac{AV}{K+HV^2}\,, \tag{27}$$

the corresponding characteristic function assumes the form:

$$D_{\mathrm{c}}(\lambda):=\left(1+\tilde{D}U\mathrm{e}^{-\lambda\tilde{\tau}}\right)\lambda^2+\left(\tilde{P}U+\tilde{D}\right)\mathrm{e}^{-\lambda\tilde{\tau}}\lambda+\tilde{P}\mathrm{e}^{-\lambda\tilde{\tau}}-1=0\,. \tag{28}$$

This equation has infinitely many complex roots. The steady-state rectilinear motion is asymptotically stable if and only if all of the characteristic exponents are situated in the left-half of the complex plane. The limit of stability is where characteristic roots are located at the imaginary axis for some particular system parameters.

Two different types of stability boundaries can be distinguished: a saddle-node (SN) bifurcation may occur when the real and imaginary parts of a characteristic root are zero, and a Hopf bifurcation when a pair of characteristic roots is pure complex. In our model, saddle-node bifurcations may occur if

$$D_{\mathrm{c}}(\lambda=0)=0\quad\Rightarrow\quad\tilde{P}-1=0\,. \tag{29}$$

The critical proportional gains are a subset of the gains

$$\tilde{P}_{\mathrm{SN}}=1\,. \tag{30}$$

In case of a Hopf bifurcation, the critical characteristic exponent is a pure imaginary number $\lambda_{\mathrm{H}}=\pm\mathrm{i}\omega$, $\omega\in\mathbb{R}^+$ where ω is the dimensionless angular frequency of the resultant self-excited vibration. After its substitution, the characteristic equation

$$D_{\mathrm{c}}(\lambda=\mathrm{i}\omega)=0$$

can be separated into real and imaginary parts according to the D-subdivision method:

$$\left(\tilde{P}-\tilde{D}U\omega^2\right)\cos(\omega\tilde{\tau})+\left(\tilde{D}+\tilde{P}U\right)\omega\sin(\omega\tilde{\tau})-1-\omega^2=0\,, \tag{31a}$$
$$\left(\tilde{D}+\tilde{P}U\right)\omega\cos(\omega\tilde{\tau})-\left(\tilde{P}-\tilde{D}U\omega^2\right)\sin(\omega\tilde{\tau})=0\,. \tag{31b}$$

Then from Eq. (31) the critical dimensionless gains can be calculated in closed form:

$$\tilde{P}_{\mathrm{H}}=\left(1+\omega^2\right)\frac{\cos\left(\omega\tilde{\tau}\right)+U\omega\sin\left(\omega\tilde{\tau}\right)}{1+U^2\omega^2}\,, \tag{32a}$$
$$\tilde{D}_{\mathrm{H}}=\left(1+\omega^2\right)\frac{\sin\left(\omega\tilde{\tau}\right)-U\omega\cos\left(\omega\tilde{\tau}\right)}{\omega\left(1+U^2\omega^2\right)}\,. \tag{32b}$$

By means of Eq. (30) and Eq. (32) one can construct the stability chart in the plane of the rescaled dimensionless control gains $\tilde{P}-\tilde{D}$ (see figure 3). The saddle-node (SN) bifurcation boundary can be interpreted as a vertical line at $\tilde{P}=\tilde{P}_{\mathrm{SN}}$. When this stability boundary is crossed from right to left, the steady-state rectilinear motion loses its stability without vibrations, that is, we have static instability for $\tilde{P}<\tilde{P}_{\mathrm{SN}}$. The stability boundary characterized by Eq. (32) has a starting point at $\omega=0$ on the SN bifurcation line. If this D-curve is crossed, a pair of complex conjugate characteristic roots crosses the imaginary axis of the complex plane. In figure 3, numbers show the numbers of the characteristic roots that have positive real parts [20]; only the small shaded parameter domain is stable.

In case of the stability analysis of NDDEs, a stability boundary can also be detected where infinitely many characteristic roots cross the imaginary axis of the complex plane [20]. Since, the eigenvalues of the coefficient matrix $\mathbf{T}_1$ of the highest delayed derivative term in the equation of motion (25) are 0 and $\tilde{D}U$, these kinds of "infinitely unstable" domains are found at

$$\left|\tilde{D}\right|>\frac{1}{U}\,. \tag{33}$$

It can be proved that the stable domain and the "infinitely unstable" domain are adjacent if and only if $U=1$. All the above mathematical results can be observed in figure 3.

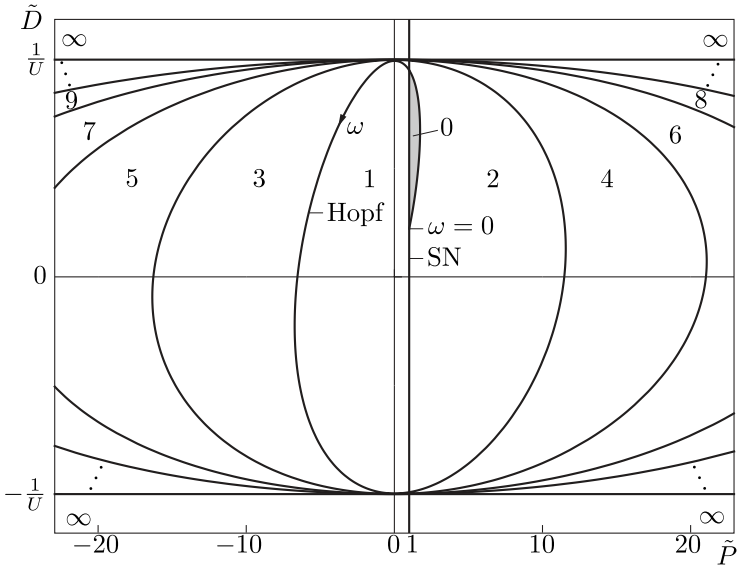

Figure 3: Stability chart in the plane of the rescaled dimensionless proportional gain $\tilde{P}$ and the rescaled dimensionless differential gain $\tilde{D}$ for fixed dimensionless delay $\tilde{\tau}$ =1 and rescaled dimensionless speed $U = 0.65$. The region of stability is shaded. The numbers refer to the numbers of the characteristic roots with positive real parts in the corresponding domains of the parameter plane. The Hopf and SN labels refer to the types of possible bifurcations along the stability boundary: Hopf and saddle-node, respectively.

4 Physical interpretation of stability chart

Let us investigate the effect of the skater's reflex time on stability. By means of the stability chart in figure 3, it can be shown that there is no stable domain if the D-curve (32) leaves the vertical SN bifurcation line to the left. Since $\mathrm{d}\tilde{P}_\mathrm{H}/\mathrm{d}\omega|_{\omega=0} = 0$, the necessary and sufficient condition for the existence of a stable domain can be written as

$$\left.\frac{\mathrm{d}^2\tilde{P}_\mathrm{H}}{\mathrm{d}\omega^2}\right|_{\omega=0} = 1 - U^2 + U\tilde{\tau} - \frac{1}{2}\tilde{\tau}^2 > 0\,. \tag{34}$$

This means that

$$\max\left(0; \tilde{\tau}_{\mathrm{cr}2}\right) < \tilde{\tau} < \tilde{\tau}_{\mathrm{cr}1}\,, \tag{35}$$

where

$$\tilde{\tau}_{\mathrm{cr}1,2} = U \pm \sqrt{2 - U^2}\,. \tag{36}$$

It is easy to prove that the maximum of $\tilde{\tau}_{\mathrm{cr}1}$ is $\tilde{\tau}_\mathrm{c} = 2$. This means that there is no stable parameter domain for any parameter combination if

$$\tau > \tau_\mathrm{c} = \frac{2}{\omega_1} = 2\sqrt{\frac{h}{g}} = \frac{T}{\pi}\,, \tag{37}$$

where T is the time period of the pendulum representing the skater "hanging downwards" for $V = 0$ and $k_\mathrm{t} = 0$. This critical reflex delay is $\sqrt{2}$ times larger than the similarly interpreted critical reflex delay of a simple human balance model in [12]. For zero longitudinal speed, we get back the critical delay $\tau_\mathrm{cr} = T/(\sqrt{2}\pi) < \tau_\mathrm{c}$ for the simple human balancing model without the skateboard. This implies that riding on a skateboard is easier in certain speed ranges than standing on the ground; in other words, skateboarding can be managed with larger reflex delay than standing. However, note that the vertical position of the skater is stabilizable below the critical reflex delay in some speed ranges for certain system parameter combinations.

A dimensionless stability chart can be constructed without using fixed values for the system parameters (see figure 4). The dependence of U on the dimensionless speed V is plotted in the upper panel of the figure, parametrized by the dimensionless position of the skater A, the dimensionless height of the skater H and the dimensionless stiffness parameter K. The shaded domain in the lower panel indicates where the necessary and sufficient stability condition (35) is satisfied, that is, where the systems can be stabilized by appropriately chosen $P - D$ parameters. The right and the left sides of this stability chart mathematically belong to the cases where AV is positive or negative, respectively. Due to the symmetry of the system in the standing position of the skater and the direction of the motion (sign of the longitudinal speed v), we consider cases when the dimensionless speed V is positive only while we assume that the parameter A can be either positive or negative

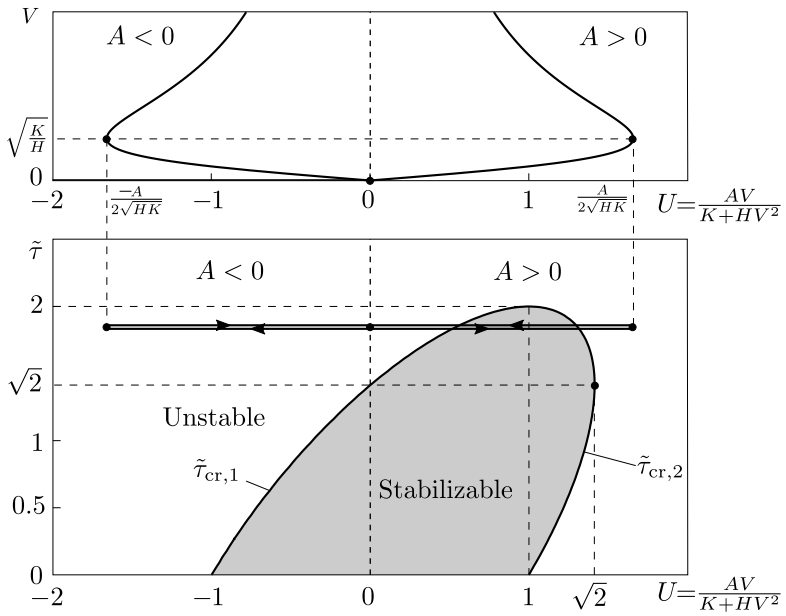

Figure 4: Critical reflex delay.

referring to cases when the skater stands ahead ($A > 0$) or behind ($A < 0$) of the centre of the board. Thus, the left side of figure 4 corresponds to behind standing while the right one belongs to the ahead standing.

For the fixed dimensionless time delay $\tilde{\tau}$ =1.8 in the upper panel of figure 4, thick horizontal segments can be swept along by means of the dimensionless speed V. The end points of these lines are characterized by parameters A, H and K, while the exact position within these lines is determined by V. As a consequence, different types of stability behaviour can occur as the speed increases. Consider the case illustrated in figure 4 for $A > 0$ (that is, the skater stands ahead) when the linear stability properties change four times as the speed increases from zero to infinity. This is always true if the dimensionless time delay is $\sqrt{2} < \tilde{\tau} < 2$ and the ratio A^2/HK is sufficiently large. This will explain the wavy shape of the upper stability boundary in figure 5 for a case study. For this dimensionless time delay, the rectilinear motion is unstable independently from the control gains if the skater stands behind the centre of the board ($A < 0$). Several other intricate stability properties can be explored in the system which will be discussed in the subsequent section using realistic physical parameters instead of the dimensionless ones.

5 A case study

In order to explain the physical interpretation of the results, especially the dependence of stability on the speed v and on the reflex time τ, a case study is presented using realistic parameters. Consider the height and the mass of the skater as $2h = 1.7$ m and $m = 75$ kg, respectively; the length of the board is $2l = 0.787$ m and the rake angle in the skateboard wheel suspension system is 27 degree, i.e. $\kappa = 0.47$ rad. These parameters lead to $\omega_1 = 3.397$ rad/s and corresponding time period of oscillation $T = 1.85$ sec.

Two different cases are assumed in this study; first, when the skater stands ahead of the centre of the board ($a > 0$), second, when the skater stands behind ($a < 0$). The qualitative difference of these cases is especially relevant because the position of the skater can be changed during riding. figure 5 shows the variation of the critical time delay versus the longitudinal speed for torsional stiffness $k_\mathrm{t} = 100$ Nm/rad of the suspension system. Panel (a) and (b) correspond to $a = 0.1$ m and $a = -0.1$ m, respectively. As it can be observed in the figure, the maximal time delay, by which the system can be stabilized, is larger for any speed when the skater stands ahead of the centre point of the board. However, in case of smaller reflex delay, the stabilization of the rectilinear motion is still possible even when the skater stands behind the centre of the board. Earlier mechanical models without control cannot explain such dynamic behaviour of the skateboard. For example, [3] concluded that the rectilinear motion cannot be stable in case of $a < 0$ for any speed.

Another interesting part of figure 5 is that the maximal allowable reflex delay tends to $\sqrt{2}/\omega_1 = 0.42$ sec as v increases. Namely, for very high speeds, the position of the skater on the board does not influence the required reflex delay.

The stability properties are even more interesting when the torsional stiffness of the wheel suspension system is small, which is the usual case in practice. For example, the reduced torsional stiffness can improve the manoeuvrability of the skateboard since smaller control efforts are required by the skater to tilt the board

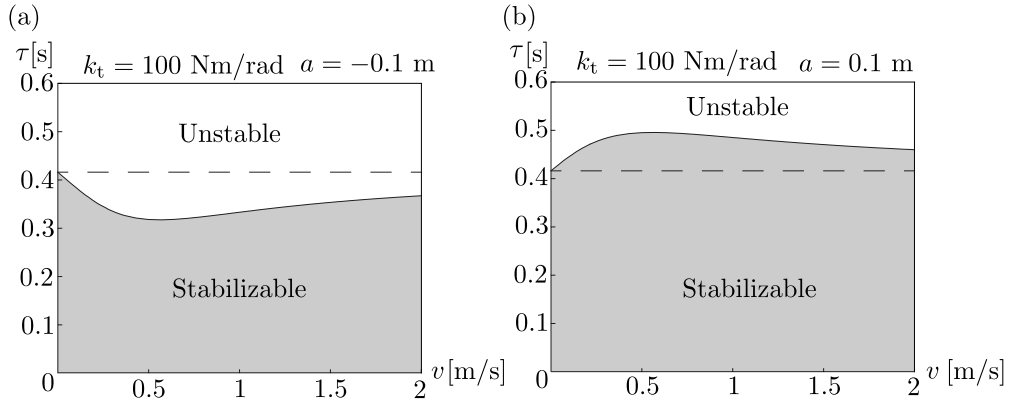

Figure 5: Required time delay τ as a function of the longitudinal speed v, with large torsional spring stiffness $k_t = 100 Nmrad^{-1}$ in the suspension. Panel (a): skater stands behind ($a < 0$), panel (b): skater stands ahead ($a > 0$) of the centre of the board.

and to turn the wheels. Figure 6 shows the variation of the allowable time delay versus the speed for different stiffness values. For the realistic $k_t = 5$ Nm/rad value, it can be observed that the minimum of the time delay curve goes to zero when the skater stands behind the centre of the board (figure 6a). As a consequence, the rectilinear motion cannot be stabilized in a specific speed range of speed even by zero time delay in the control loop. If the skater stands ahead of the centre (see panel (b) in figure 6), a lower limit occurs for the reflex time, which means that there is a speed range, where the skater cannot stabilize the rectilinear motion short reflex time, but can stabilize with larger one. This specific counter-intuitive property of delayed oscillators was recognised in several publications on time delay systems [21].

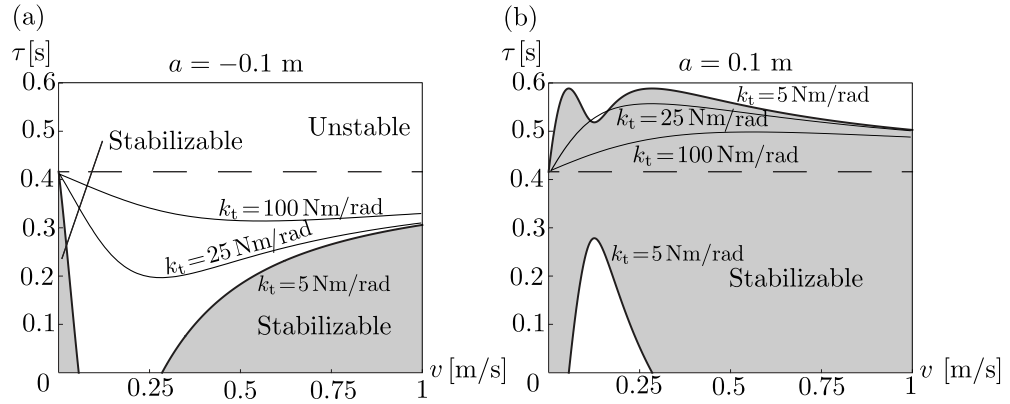

Figure 6: Required time delay τ as a function of the longitudinal speed v, with lower torsional spring stiffness in the suspension. Panel (a): skater stands behind ($a < 0$), panel (b): skater stands ahead ($a > 0$) of the centre of the board.

As was mentioned, having a properly chosen time delay is not sufficient to produce stable rectilinear motion; the control gains have to be tuned. The effect of the longitudinal speed is investigated in figure 7, where $\tau = 0.294$ sec corresponding to $\tilde{\tau}$ =1. The choice of this value is in good agreement with literature (see [22, 23]). The D-curves are constructed in the $p - d$ parameter plane for different longitudinal speeds, (see panel (a) of figure 7). Dashed and solid lines correspond to the cases when the skater stands behind and ahead of the centre of the board, respectively. So it can clearly be seen that the latter case is much more advantageous: the corresponding stable domains are much larger.

Another interesting point in figure 7 is how the location of the stable parameter domain changes with respect to the speed of the board. Namely, the stable domain tends to the origin ($p = 0$, $d = 0$) as the speed increases. As a consequence, the skater has to tune the control parameters to catch a very narrow stable parameter domain at high speeds. Due to the fact that the skater has to use very small control gains, the dead-zones in the human control become relevant. The skater cannot apply close to zero control torque and cannot even sense very small tilting angles of the board. This may lead to so-called micro-chaotic oscillations which can still be considered as practically stable [23].

In figure 7, the frequency $f = \omega_1\omega/(2\pi)$ of the emerging self-excited vibration is plotted along the Hopf-type (dynamic) stability boundaries. It is below 1 Hz ($\omega_1\omega < 2\pi$ rad/s), which is in good agreement with

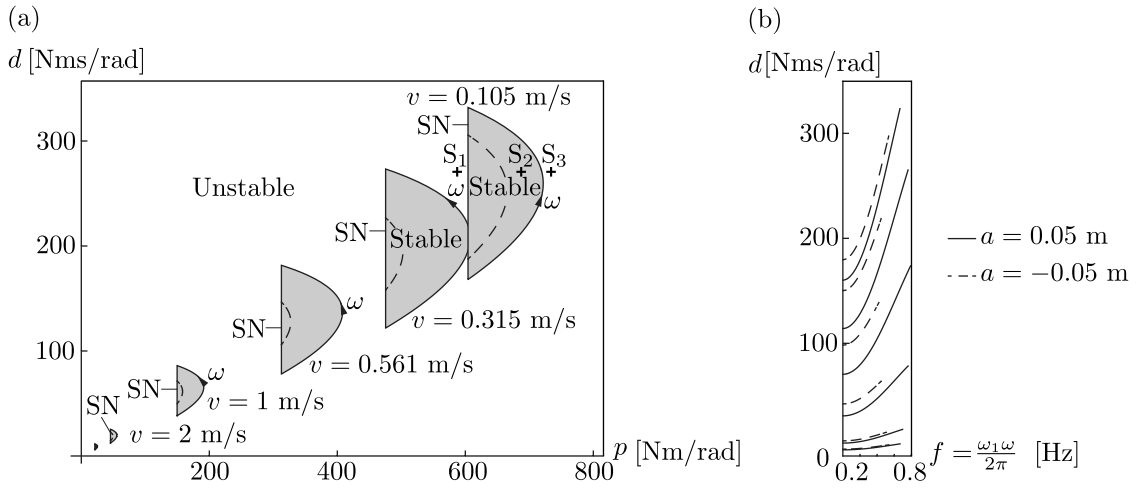

Figure 7: Stability charts for various longitudinal speeds: (a) stability charts for *pd* control gains, (b) frequencies along the dynamic stability boundaries. The points S_i indicate in (a) parameters sets for numerical simulations in figure 8.

practical observations when skaters start oscillating after loss of stability. Numerical simulation results on the time histories of deflection angles φ and β of the skater and the board, respectively, are presented in figure 8 for parameter sets denoted by S_1, S_2 and S_3 in figure 7.a. The rectilinear motion is statically unstable for S_1, stable for S_2, and dynamically unstable for S_3 as shown by panels (a), (b) and (c) of figure 8, respectively. One can observe that the board and the skater oscillate in phase. This is the same for other longitudinal speeds since the time delay is 6-8 times smaller than the smallest time period of the emerging self-excited vibration (see figure 7.b).

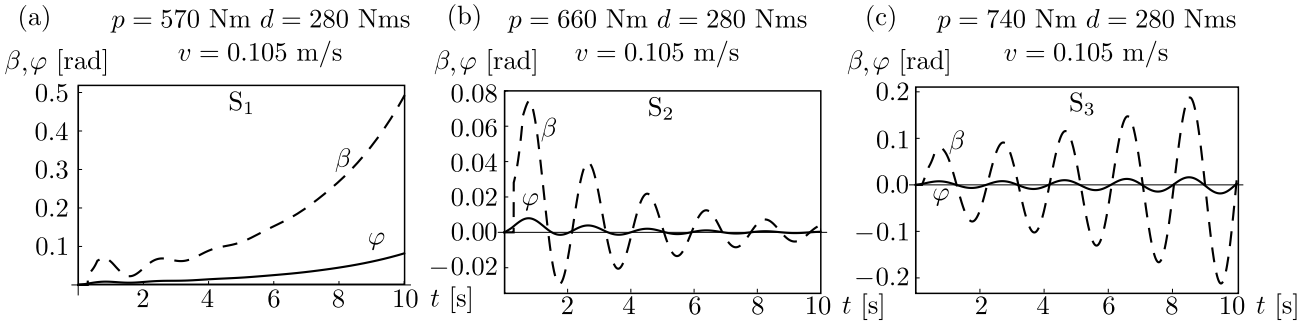

Figure 8: Numerical simulation results on the time histories of deflection angles φ and β of the skater and the board, respectively; panel (a) shows static instability at parameter point S_1 of figure 7.a., panel (b) shows a stable case at S_2, and panel (c) shows dynamical instability at S_3.

The loss of stability also can be explained by parameter sensitivity, namely, the choosing of appropriate control gains in a real application is much difficult as the stable domain is smaller. Figure 9 provides some information about the dependency of stable areas on the longitudinal speed. The plotted curves show the areas of the stable domains relative to the stable domain at zero speed (A_r). The larger the speed, the smaller the stable parameter domain. Note the logarithmic scale on the vertical axis, so the possibility of choosing stable control gains decreases significantly as the speed increases.

6 Conclusion

A mechanical model of the skateboard-skater system was introduced, in which the effect of the human balancing was taken into account by means of a linear PD controller. As a relevant parameter of the model, the reflex time of the skater was also considered as a time delay in the control loop. The stability of the rectilinear motion of the skateboard was analysed and stability charts were composed with special attention to the reflex time, longitudinal speed and control gains.

Critical time delays were calculated for realistic parameters. It was shown that skateboarding can be performed in certain speed ranges with $\sqrt{2}$ times larger time delays than the balancing of quiescent standing on the ground. This is caused by in the special steering mechanism of the wheel suspensions. The effect of

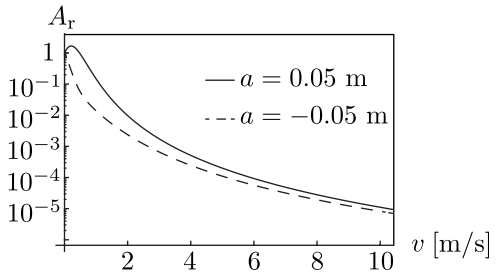

Figure 9: The relative area of the stable domains with respect to the longitudinal speed for the cases when the skater stands behind or ahead the centre of the board

the skater's position on the board was also investigated and it was established that it is more advantageous if the skater stands ahead of the centre of the board: large reflex delay is tolerated, and the control gains can be chosen from larger parameter domains.

Our analysis also showed that low stiffness of the skateboard's suspension system can lead to instability in some speed ranges if the skater reacts with small delay. This surprising phenomenon confirms that there exist delayed oscillators which can be stabilized with increasing the delay while they are unstable for small or even for zero delay.

In human balancing or stick balancing models, it was shown by Insperger et al. in [24] and [23] respectively, that a delayed acceleration feedback additional to the PD controller (a proportional-derivative-acceleration (PDA) controller) improves stability. However, in case of the skateboard-skater system, PDA controller leads to advanced delay-differential equations and consequently the rectilinear motion is unstable for any parameter setup. Nevertheless, many other control strategies are developed for time delayed systems with different levels of robustness (see, for example, [25]), which is to be studied in the future.

The constructed stability charts also explain the loss of stability of skateboarding at high speeds. The stable parameter domain of the control gains reduces as the speed increases and the decreasing stable domain tends towards the origin. As a consequence, the skater must decrease the control gains at large speeds, which can amplify the effects of the dead-zones of the human control. In human balancing models, the existence of dead-zones are also suspected as the reason of transient-chaotic vibration around linearly unstable equilibria with large surviving times [23]. Similar phenomena are expected in case of skateboarding which are also possible areas of future research.

Acknowledgement: This research was partly supported by the Janos Bolyai Research Scholarship of the Hungarian Academy of Sciences and by the Hungarian National Science Foundation under grant no. OTKA PD105442.

References

[1] Hubbard M. Lateral dynamics and stability of the skateboard. Journal of Applied Mechanics. 1979;46:931–936. doi: 10.1115/1.3424680

[2] Hubbard M. Human control of the skateboard. Journal of Biomechanics. 1980;13(9):745–754. doi: 10.1016/0021-9290(80)90236-5

[3] Kremnev AV, Kuleshov AS. Dynamics and Simulation of the Simplest Model of a Skateboard. Europien Nonlinear Dynamics Conference. 30 June 4 July, 2008, Saint Petersburg, Russia

[4] Wisse M, Schwab AL. Skateboards, Bicycles, and Three-dimensional Biped Walking Machines: Velocity-dependent Stability by Means of Lean-to-yaw Coupling. The international Journal of Robotics Research. 2005 jun;24(6):417–429. doi: 10.1177/0278364905053803

[5] Silva MF, Machado JT. A literature review on the optimization of legged robots. Journal of Vibration and Control. 2012;18(12):1753–1767. doi: 10.1177/1077546311403180

[6] Silva MF, Machado JT. A historical perspective of legged robots. Journal of Vibration and Control. 2007;13(9-10):1447–1486. doi: 10.1177/1077546307078276

[7] Kooijman J, Meijaard J, Papadopoulos JM, Ruina A, Schwab A. A bicycle can be self-stable without gyroscopic or caster effects. Science. 2011;332(6027):339–342. doi: 10.1126/science.1201959

[8] Wang EX, Zou J, Liu Y, Fan Q, Xiang Y. Symbolic derivation of nonlinear benchmark bicycle dynamics with holonomic and nonholonomic constraints. In: 16th International IEEE Conference on Intelligent Transportation Systems (ITSC 2013). 06 Oct 09 Oct 2013, The Hague, Netherlands pp. 316–323. doi: 10.1109/ITSC.2013.6728251

[9] Chiementin X, Rigaut M, Crequy S, Bolaers F, Bertucci W. Hand-arm vibration in cycling. Journal of Vibration and Control. 2012;p. 1077546312461024. doi: 10.1177/1077546312461024

[10] Rosatello M, Dion Jl, Renaud F, Garibaldi L. The Skateboard Speed Wobble. In: Proceedings of ASME 11th International Conference on Multibody Systems, Nonlinear Dynamics, and Control. 2-5 August, 2015, Boston, Massachusetts, USA, 2015. p. 1–10. doi: 10.1115/DETC2015-47326

[11] Milton JG, Solodkin A, Hluštík P, Small SL. The mind of expert motor performance is cool and focused. NeuroImage. 2007;35(2):804–813. doi: 10.1016/j.neuroimage.2007.01.003

[12] Stepan G. Delay effects in the human sensory system during balancing. Phil Trans Roy Soc A. 2009;367(1891):1195–1212. doi: 367:11951212

[13] Chagdes JR, Haddad JM, Rietdyk S, Zelaznik HN, Raman A. Understanding the Role of Time-Delay on Maintaining Upright Stance on Rotational Balance Boards. In: Proceedings of ASME 11th International Conference on Multibody Systems, Nonlinear Dynamics, and Control. 2-5 August, 2015, Boston, Massachusetts, USA, 2015. p. 1–7. doi: 10.1115/DETC2015-47857

[14] Gantmacher F. Lectures in Analytical Mechanics. Moscow: MIR Publiser; 1975.

[15] Varszegi B, Takacs D, Stepan G. Skateboard: a Human Controlled Non-Holonomic System. In: Proceedings of ASME 11th International Conference on Multibody Systems, Nonlinear Dynamics, and Control. 2-5 August, 2015, Boston, Massachusetts, USA, 2015. p. 1–6. doi: 10.1115/DETC2015-47512

[16] Takacs D., Stepan G. Contact patch memory of tyres leading to lateral vibrations of four-wheeled vehicles. Philosophical Transactions of the Royal Society A. 2013; 371(1993) doi: 10.1098/rsta.2012.0427

[17] Ispolov, Y., and Smolnikov, B., Skateboard dynamics. Computer Methods in Applied Mechanics and Engineering. 1996; 131(3-4):327-333 doi: 10.1016/0045-7825(95)00932-9

[18] Bloch AM. Nonholonomic mechanics and control. Springer; 2003. doi: 10.1007/b97376

[19] Kane TR, Levinson DA. Dynamics, theory and applications. Internet-First University Press. Ithaca, N.Y

[20] Stepan G. Retarded dynamical systems: stability and characteristic functions. Longman, London co-published with Wiley, New York; 1989.

[21] Insperger T, Stepan G. Semi-Discretization for Time-Delay Systems. Springer; 2011. doi: 10.1007/978-1-4614-0335-7

[22] Chagdes JR, Rietdyk S, Jeffrey MH, Howard NZ, Raman A. Dynamic stability of a human standing on a balance board. Journal of Biomechanics. 2013;46(15):2593–2602. doi: 10.1016/j.jbiomech.2013.08.012

[23] Insperger T, Milton JG. Sensory uncertainty and stick balancing at the fingertip. Biological cybernetics. 2014 feb;108(1):85–101. doi: 10.1007/s00422-013-0582-2

[24] Insperger T, Milton J, Stépán G. Acceleration feedback improves balancing against reflex delay. Journal of the Royal Society Interface. 2013;10(79):20120763. doi: 10.1098/rsif.2012.0763

[25] Molnar TG, Insperger T. On the robust stabilizability of unstable systems with feedback delay by finite spectrum assignment. Journal of Vibration and Control. 2016;22(3):649–661. doi: 10.1177/1077546314529602